Author/s:
Zanker, D;Pang, K;Oveissi, S;Lu, C;Faou, P;Nowell, C;Mbogo, GW;Carotta, S;Quillici, C;Karupiah, G;Hibbs, ML;Nutt, SL;Neeson, P;Puthalakath, H;Chen, W

Title:
LMP2 immunoproteasome promotes lymphocyte survival by degrading apoptotic BH3-only proteins

Date:
2018-10-01

Citation:
Zanker, D., Pang, K., Oveissi, S., Lu, C., Faou, P., Nowell, C., Mbogo, G. W., Carotta, S., Quillici, C., Karupiah, G., Hibbs, M. L., Nutt, S. L., Neeson, P., Puthalakath, H. & Chen, W. (2018). LMP2 immunoproteasome promotes lymphocyte survival by degrading apoptotic BH3-only proteins. Immunology and Cell Biology, 96 (9), pp.981-993. https://doi.org/10.1111/imcb.12163.

PROFESSOR WEISAN CHEN (Orcid ID : 0000-0002-5221-9771)

Article type : Original Article

BIOLOGICAL SCIENCES: CELL BIOLOGY

LMP2 immunoproteasome promotes lymphocyte survival by degrading apoptotic BH3-only proteins

Damien Zanker[a], Kenneth Pang[b,d,e,f], Sara Oveissi[a], Chunni Lu[a], Pierre Faou[a], Cameron Nowell[c], George Williams Mbogo[a], Sebastian Carotta[b], Cathy Quillici[c], Guna Karupiah[g], Margaret Hibbs[h], Stephen L Nutt[b], Paul Neeson[i], Hamsa Puthalakath[a], Weisan Chen[a].

[a] La Trobe Institute of Molecular Science, La Trobe University, Bundoora, VIC, 3086, Australia.

[b] The Walter and Eliza Hall Institute of Medical Research, 1G Royal Melbourne Hospital, Parkville, VIC, 3010, Australia.

[c] Ludwig Institute for Cancer Research, Royal Melbourne Hospital, Parkville, VIC 3004, Australia.

[d] Department of Paediatrics, University of Melbourne, Parkville, Australia

[e] Department of Psychiatry, University of Melbourne, Parkville, Australia

[f] Murdoch Children's Research Institute, Parkville, Australia

[g] Australian National University, Canberra, Australia

[h] Department of Immunology, Monash University, AMREP Melbourne 3004 Victoria, Australia

[i] Peter MacCallum Cancer Centre, East Melbourne, VIC, 3002, Australia.

Running title: Immunoproteasome promotes lymphocyte survival

Corresponding author:
Professor Weisan Chen, La Trobe Institute of Molecular Science, La Trobe University, Bundoora, VIC, 3086, Australia. +61394793961, weisan.chen@latrobe.edu.au

Keywords: lymphocyte differentiation, T cell development, immunoproteasome, NFκB, survival, LMP2, BIM.

ABSTRACT

The role of the immunoproteasome is perceived as confined to adaptive immune responses given its ability to produce peptides ideal for MHC Class-I binding. Here, we demonstrate that the immunoproteasome subunit, LMP2, has functions beyond its immunomodulatory role. Using LMP2-deficient mice, we demonstrate that LMP2 is crucial for lymphocyte development and survival in the periphery. Moreover, LMP2-deficient lymphocytes show impaired degradation of key BH3-only proteins, resulting in elevated levels of pro-apoptotic BIM and increased cell death. Interestingly, LMP2 is the sole immunoproteasome subunit required for BIM degradation. Together, our results suggest LMP2 has important housekeeping functions and represents a viable therapeutic target for cancer.

INTRODUCTION

Regulation of protein homeostasis is a key biochemical process within a cell. New protein synthesis requires a constant stream of amino acids, while the clearance of misfolded proteins is crucial to negate cellular stress responses and ultimately cellular apoptosis [1]. Much of this protein degradation and clearance occurs within a multi-subunit complex known as the proteasome that exists in several isoforms including a 20S form and a larger 26S version that contains additional ubiquitin-specific subunits [2]. As well as its homeostatic role, the proteasome shapes cellular function not only by terminating the activity of ubiquitinated proteins, but also by cleaving pro-proteins to liberate their active form [3]. Finally, since the majority of proteins within a cell undergo proteasome-dependent degradation, the resultant peptide catalogue forms an important reservoir for the adaptive immune system to elicit cytotoxic $CD8^+$ T cell (T_{CD8+}) responses via MHC class I presentation [4] thereby facilitating the clearance of virus infected cells and tumours [5].

The 20S proteasome is comprised of four stacked heptameric rings. The two inner rings contain the catalytically active beta subunits, β_1, β_2 and β_5 [6], which can be substituted in different circumstances. The best known of these, the immunoproteasome (IP), has a reported specialised role in antigen presentation. Specifically, the IP has substitutions of all three catalytic β-subunits, which are replaced by β_{1i} (LMP2), β_{2i} (LMP10) and β_{5i} (LMP7) respectively [7-10]. The IP is constitutively expressed in antigen presenting cells, such as dendritic cells, and in medullary thymic epithelial cells (mTECs) that influence negative T cell selection [11], and it is upregulated in other cell types upon exposure to anti-viral interferons [12]. Consistent with a role in antigen presentation, the IP demonstrates an altered cleavage pattern that preferentially creates hydrophobic and basic C-terminal residues, which are frequently used as C-terminal anchor residues for MHC-I binding [13, 14]. In this way, the IP is generally believed to enhance T_{CD8+} cell responses [15].

However, this notion is likely to be overly simplistic. For example, the IP was reported also to inhibit some immunogenic peptide generation [16]. Moreover, it has been demonstrated that the overall peptide repertoire generated by the immuno- and housekeeping proteasome is largely similar, with the major difference being the enhanced degradation rate of the former [17]. Finally, it has been demonstrated that there are hybrid versions of the immuno- and housekeeping proteasomes, which casts doubt on their perceived functional dichotomy [18, 19].

Consistent with this functional blurring of the immuno- and housekeeping proteasome, genetic defects in individual IP subunits cause systemic disease that cannot be readily explained by a role in antigen presentation alone. For example, homozygous mutations in human LMP7 cause Nakajo-Nishimura syndrome, which is a systemic autoinflammatory disorder believed to arise due to a failure to breakdown ubiquitinated and oxidated proteins [20]. Similarly in mice, genetic loss of LMP7 mice causes accumulation of polyubiquitinated proteins and oxidative stress [21]. Strikingly, several human diseases, including multiple myeloma (MM), gastric cancer, Huntington's Disease, Alzheimer's Disease and amyotrophic lateral sclerosis, have increased IP levels or are associated with subunit polymorphisms [22-26]. These observations are also hard to reconcile with the canonical role of IPs in antigen presentation.

In this study, we present a newly described housekeeping role for the LMP2 IP subunit. Specifically, we found that loss of LMP2 in mice results in cellular protein dysregulation in developing and peripheral lymphocytes, which ultimately causes apoptosis due to the failure to degrade pro-apoptotic proteins.

RESULTS

LMP2$^{-/-}$ mice exhibit reduced lymphocyte numbers in both the thymus and spleen

Decreased T_{CD8+} numbers in the thymus and periphery of IP subunit-deficient mice have been reported previously [27, 28]. To confirm previous results, primary and secondary lymphoid organs were first collected from wild type C57BL6/J (B6) mice and each of three IP subunit-deficient (LMP2$^{-/-}$, LMP7/LMP10$^{-/-}$ and LMP10$^{-/-}$) strains and total cell numbers were enumerated. As shown in Figure 1A, thymic cell numbers were decreased in the IP subunit-deficient strains compared to B6 mice. However, as previously reported, LMP2$^{-/-}$ animals were the only strain that displayed reduced splenic cellularity [15, 29], which was hard to reconcile with the general assumption that LMP2's sole role is to be incorporated in IP to facilitate antigen presentation.

To understand which splenocyte populations were affected, we analyzed the myeloid and lymphoid compartments in the spleen (Figure 1B). As expected B6, LMP7/LMP10$^{-/-}$ and LMP10$^{-/-}$ mice all displayed intact myeloid and lymphoid compartments. In contrast, mice lacking LMP2 had a pan-lymphoid deficiency, with a 50% reduction in T_{CD4+}, T_{CD8+}, NK and NKT cell numbers. As we have previously reported, LMP2$^{-/-}$ mice also exhibited a substantial decrease in CD19^{+} B cells (~80% reduction) [29].

We believe the differences we observed were likely overlooked in the original description of LMP2$^{-/-}$ mice [27] as the authors compared cell subset percentages rather than assessing absolute cell numbers. No significant difference was detected in the myeloid compartment of LMP2$^{-/-}$ mice.

The LMP2-dependent reduction in lymphocyte numbers is not a result of impaired thymic selection

The lymphocyte deficiency observed in LMP2$^{-/-}$ mice suggested the underlying mechanism was unlikely to be due to increased negative selection in the thymus as suggested previously [27], especially given the involvement of B and NK cells which develop in the bone marrow. Instead, we hypothesized that loss of LMP2 causes an intrinsic defect in lymphocyte maturation. To formally test these two possibilities in the context of T cell development, BM chimeras were generated in which B6 or LMP2$^{-/-}$ BM was injected into irradiated B6 or LMP2$^{-/-}$ recipient hosts (Groups 1-4 in Supplementary table 1). Three months later, donor-derived splenocyte subpopulations were assessed (Figure 2A). As expected, the two control groups, wild type (Ly5.1 BM→B6) and LMP2$^{-/-}$ (LMP2$^{-/-}$ BM→LMP2$^{-/-}$) mice, exhibited

similar cellular profiles as seen in their non-chimeric counterparts (Figure 1B). Interestingly, Ly5.1 BM→LMP2$^{-/-}$ mice, which were generated to assess how wild type progenitor cells develop in the LMP2$^{-/-}$ thymic selection environment, exhibited cell numbers similar to that of the control Ly5.1 BM→B6 mice. This indicated that the LMP2$^{-/-}$ thymic environment is able to select normal numbers of T lymphocytes, and suggested that an intrinsic T cell defect might exist in LMP2$^{-/-}$ animals. Indeed, when LMP2$^{-/-}$ progenitor cells were exposed to a wild type thymic environment (LMP2$^{-/-}$ BM→Ly5.1), we observed reduced lymphocyte numbers similar to that in the LMP2$^{-/-}$ BM→LMP2$^{-/-}$ controls, confirming that the defect is intrinsic to either lymphocyte progenitors and/or the differentiating LMP2$^{-/-}$ thymocytes.

Interestingly, when the relative chimerism in the spleen was assessed at three months by measuring the proportion of donor T cells we found that LMP2$^{-/-}$→ Ly5.1 mice displayed very poor donor cell engraftment (35.34% +/- 2.19%), unlike the other three groups which all showed >90% donor cell contribution (Supplementary table 1). To build upon these results, mixed BM chimeras were generated (Supplementary table 1: Groups 5 and 6), using Ly5.2^{+} LMP2$^{-/-}$: Ly5.1^{+} donors at either a 1:1 or 5:1 ratio in Thy1.1^{+} irradiated recipients. This experimental setup enabled a direct comparison of wild type and LMP2 donor cells as they encountered the same thymic selection environment. Interestingly, in mice that received equal numbers of LMP2$^{-/-}$ and wild type progenitors, approximately 99% of donor thymocytes recovered were derived from wild type donor progenitors (Figure 2B). Moreover, increasing the LMP2$^{-/-}$: wild type donor cell ratio to 5:1 failed to improve LMP2$^{-/-}$ cell engraftment (Figure 2B).

LMP2$^{-/-}$ thymocytes show impaired developmental transition and increased apoptosis at the pre-TCR signaling DN3 stage

The above results indicated that LMP2$^{-/-}$ cells had an intrinsic defect in T cell development, which we initially hypothesized might be due to a problem in progenitor cells. We therefore enumerated hematopoietic stem cells (HSC; Lin^{neg} c-kit^{+} Sca-1^{+}), common lymphoid progenitors (CLP; Lin^{neg} c-kit^{-} Sca-1^{+}) and, as a control, common myeloid progenitors (CMP; Lin^{neg} c-kit^{+} Sca-1^{-}) [30, 31] . Notably, each population was comparable in number between LMP2$^{-/-}$ and B6 animals (Figure 2C), indicating that the observed reduction in T cell number in these mice was not explained by progenitor cell number.

We next investigated whether a problem might exist in thymocyte differentiation by assessing various subpopulations along the thymocyte differentiation pathway (Figure 2D). Double positive (DP; small CD5^{lo} TCR^{lo}), CD4 single positive (SP) and CD8 SP cell numbers were

all decreased in LMP2$^{-/-}$ mice, suggesting an early developmental issue upstream of the DP stage. Moreover, while early double negative (DN) populations DN1-3 were similar in number compared to those in B6, DN4 numbers were significantly reduced implying that there is a problem in the transition from the DN3 to DN4 stage, a checkpoint known as 'β-selection' which corresponds to initiation of pre-TCR signaling. During this process, DN3 cells that have been successfully selected undergo rapid proliferation and an increase in cell size ('L' (large) stage), which allows them to be readily distinguished from the rest of the DN3 population ('E' (expected) stage) [32]. Consistent with a problem in β-selection, LMP2$^{-/-}$ mice possessed fewer DN3 'L' cells compared to B6 mice, but similar numbers of DN3 E cells (Supplementary figure 1A).

To further examine β-selection in LMP2$^{-/-}$ thymocytes, an OP9-DL1 culture system, in which thymocytes develop *in vitro*, was employed [33]. Following 15 days of culture, B6 HSCs progressed to the DP stage of thymic development. In contrast, most LMP2$^{-/-}$ HSCs failed to progress past the DN3 stage ($CD4^-CD8^-CD44^-CD25^+$) in the LMP2$^{-/-}$ cultures (Supplementary figure 1B-D).

Decreased thymocyte number could result from either impaired thymocyte proliferation and/or increased apoptosis. To assess thymocyte proliferation, we CFSE labeled B6 and LMP2$^{-/-}$ thymocytes and non-specifically stimulated with Concanavalin A for 72hrs, and no difference was observed (Supplementary figure 1E). To assess apoptosis throughout thymocyte development, we used Annexin V staining. Interestingly, LMP2$^{-/-}$ thymocytes demonstrated increased rates of apoptosis at developmental checkpoints, specifically during the E stage of DN thymocyte development (Supplementary figure 1F). Classical NFκB pathway activation is critical for survival of differentiating lymphocytes, especially those during DN3 stage as preTCR expression triggers NFκB signaling pathway [32, 34, 35]. We therefore isolated DN3 and DN4 thymocytes from LMP2$^{-/-}$ and B6 animals, confirmed their IP subunit expression by western blot (WB) (Supplementary figure 2A) and showed reduced IκBα degradation upon TNFα activation (data not shown). These results demonstrate a similar phenotype to developing B cells obtained from LMP2$^{-/-}$ mice that we have reported previously (Supplementary figure 2B) [29].

LMP2$^{-/-}$ lymphocytes show survival defects beyond the DN3 stage of development

Next we wished to explore whether LMP2$^{-/-}$ T cells beyond the DN3 thymocyte stage also display a defect in survival. To begin, we sought to determine whether mature T cells also express LMP2. Splenic T cells were therefore isolated and assessed for the presence of LMP2

as well as the other two IP subunits by WB. Interestingly, both T_{CD8+} and T_{CD4+} express all three IP subunits (Figure 3A and data not shown).

Before assessing survival, we again sought to determine whether mature $LMP2^{-/-}$ T cells have any defect in proliferation which might otherwise contribute to the reduced T cell numbers observed in the periphery. To do so, we first assessed the T_{CD8+} population within the spleens of B6 and $LMP2^{-/-}$ mice based on cell surface staining for CD44 and CD62L (Figure 3B) [36]. Notably, a high proportion of cells in the $LMP2^{-/-}$ spleen showed a homeostatically proliferating (ii: $CD44^+$ $CD62L^+$) phenotype, and this was accompanied by a significant reduction in the naïve ($CD62L^+$ $CD44^-$) population. Next, in order to control for potential confounding differences in T cell receptor arrangement (expression) and T cell repertoire and to facilitate *ex vivo* tracking, we bred a TCR transgenic mouse strain (F5), whose T_{CD8+} all express pre-arranged transgenic TCR specific for the H-$2D^b$-presented $NP_{366-374}$ (ASNENMDAM) - an immunodominant epitope from influenza A virus (NT60 strain), onto either $LMP2^{-/-}$ or B6 Ly5.1 background. Interestingly, $LMP2^{-/-}$-F5 TCR Tg mice exhibited widespread T and B cell deficiencies similar to our findings in $LMP2^{-/-}$ mice (Supplementary figure 2C, D). Importantly, we also confirmed that *ex vivo* isolated $LMP2^{-/-}$-F5 T_{CD8+} show a much greater tendency to homeostatically proliferate by staining with a cell proliferation dye and measuring unstimulated cell division *in vitro* (Figure 3B). We interpreted these observations as a likely compensation (albeit only partial) for the overall reduction in T_{CD8+} cell numbers in the periphery (Figure 1B). This was further confirmed by the normal $CD44^+CD62L^+$ $LMP2^{-/-}$ lymphocyte population in $LMP2^{-/-}$ bone marrow reconstituted B6 mice, in which large number of host lymphocytes survived due to the poor reconstituting capacity of the $LMP2^{-/-}$ bone marrow cells (Supplementary table 1, Supplementary figure 2E). Crucially, these data emphasized that $LMP2^{-/-}$ T cells do not appear to have an intrinsic defect in proliferation.

Next, to evaluate survival of $LMP2^{-/-}$ T cells in the periphery, we transferred equal numbers of dye-labeled T_{CD8+} from $LMP2^{-/-}$-F5 and wild type Ly5.1-F5 strains into B6 or $LMP2^{-/-}$ hosts. As shown in Figure 3C, mature $LMP2^{-/-}$-F5 TCR Tg T_{CD8+} accounted for only ~25% of the recovered donor population after 7 days in both B6 and $LMP2^{-/-}$ hosts, indicating a defect in survival that is independent of T cell repertoire. In order to determine if this survival defect is caused by increased apoptosis, Annexin V staining was assessed and found to be elevated in $LMP2^{-/-}$ peripheral T_{CD8+} (Figure 3D).

LMP2 is required to efficiently degrade BIM and other pro-apoptotic BH3-only proteins

Numerous pro-apoptotic and pro-survival proteins are degraded by the proteasome [37-40]. In particular, levels of BIM - the pro-apoptotic BH3-only protein family member that regulates the final cell death check point in developing thymocytes and peripheral T and B cells – are known to be regulated by proteasomal destruction [40, 41]. We therefore hypothesised that LMP2 is required to negate cellular apoptosis via degradation of BIM. To test this, we first decided to assess the relationship between LMP2 and BIM degradation in murine embryonic fibroblasts (MEFs). Specifically, we obtained $BIM^{-/-}$ MEFs that expressed a tamoxifen-inducible form of BIM_{EL} ($BIM^{-/-}$ BIM_{EL}), thus allowing us to control and monitor the steady-state levels of BIM_{EL} [42] and, using CRISPR/Cas9 technology, we created $LMP2^{-/-}$ $BIM^{-/-}$ BIM_{EL} MEFs to investigate BIM degradation (Supplementary figure 3). Since MEFs do not constitutively express IP subunits, LMP2 expression was induced using IFN-γ stimulation for 48hrs, while BIM expression was induced by the addition of 4-hydroxyl tamoxifen for 16h and then followed via a chase in the presence of protein synthesis inhibitor cycloheximide (CHX) for 4 hours by WB analysis. Interestingly, IFN-γ induction induced BIM degradation in wild type $BIM^{-/-}BIM_{EL}$ cells, consistent with the IP expression playing a role in BIM degradation (Figure 4A). However, since IFN-γ has a myriad effects on the cell, it was possible that this degradation was unrelated to IP expression. We therefore performed the same experiment again, but in parallel used MEFs deficient in the LMP2 subunit. Notably, loss of LMP2 drastically retarded BIM degradation (Figure 4B), demonstrating that LMP2 is crucial for efficient BIM degradation.

To investigate whether the degradation of other proteins involved in apoptosis and cell survival might be regulated by LMP2, we also used the same experimental system to examine levels of other BH3-only pro-apoptotic proteins BAX and t-BID as well as the key pro-survival protein BCL-2, all of which have previously shown to be degraded by the proteasome [37, 38, 43]. Interestingly, degradation of both BAX and t-BID was decreased in $LMP2^{-/-}$ MEFs compared to the housekeeping proteasome composition (Figure 4C, D), while no difference was observed for BCL-2 (data not shown).

$LMP2^{-/-}$ lymphocytes have increased levels of BIM and other pro-apoptotic proteins, and their impaired survival can be rescued by deletion of BIM

Taken together, the above findings suggested that loss of LMP2 tips the balance in favor of pro-apoptotic proteins within the cell and that this was likely to be important in the reduced survival of $LMP2^{-/-}$ lymphocytes, especially those past the DN3 stage in the thymus and in the periphery. To test this hypothesis, we first assessed levels of BIM, BAX and BAK in

LMP2$^{-/-}$ splenic CD8+ T and B cells via WB analysis, and observed increases in each of the proteins (Figure 4E). To demonstrate that the impaired survival of LMP2$^{-/-}$ lymphocytes is causally related to impaired BIM degradation, we next generated LMP2$^{-/-}$BIM$^{-/-}$ mice. As shown in Figure 5, LMP2$^{-/-}$ BIM$^{-/-}$ mice displayed rescue of their thymocyte and peripheral lymphocyte numbers (Figure 5A-B). Strikingly, BIM deletion in LMP2$^{-/-}$ mice also enabled LMP2$^{-/-}$ lymphocytes to survive to the same extent as their BIM$^{-/-}$ counterparts when co-transferred into a third-party host (Figure 5C).

To independently confirm the mechanistic role of BIM in driving the lymphocyte phenotype in LMP2$^{-/-}$ animals, we conducted a series of experiments involving BCL-2. BCL-2 forms anti-apoptotic complexes with BIM, thus limiting BIM's ability to activate BAX and BAK, which permeabilize the mitochondrial membrane leading to Cytochrome C release and induction of the executioner caspase cascade [44]. We therefore hypothesized that overexpression of BCL-2 should correct the survival defect in LMP2$^{-/-}$ lymphocytes by counteracting the excess levels of BIM. To test this, we crossed LMP2$^{-/-}$ mice to vav-BCL-2 transgenic mice in which the human BCL-2 coding region has been cloned under the control of the vav promoter, which drives gene expression exclusively in hematopoietic cells [45]. Notably, our previously observed defect in LMP2$^{-/-}$ DN3 → DN4 transition was ameliorated in LMP2$^{-/-}$-vav-BCL-2-Tg mice (data not shown), and these animals demonstrated similar thymocyte and peripheral lymphocyte populations compared to B6-vav-BCL-2-Tg mice (Figure 5A-B). To test the survival of these lymphocytes, we again conducted co-transfer experiments by mixing eFluor®670-labeled B6-vav-BCL-2-Tg T_{CD8+} with either LMP2$^{-/-}$ deficient or LMP2$^{-/-}$-vav-BCL-2-Tg CFSE-labeled T_{CD8+} (all CD45.2^{+}), respectively, at 1:1 ratio into third party CD45.1^{+} hosts. As shown in Figure 5D, LMP2$^{-/-}$ T_{CD8+} again survived poorly after co-transfer with B6-vav-BCL-2-Tg T_{CD8+}, while LMP2$^{-/-}$-vav-BCL-2-Tg T_{CD8+} survived equally well when they were co-transferred with those from their B6 counterparts (Figure 5D). Taken together, these results thus indicated that BIM is the final checkpoint in determining LMP2$^{-/-}$ lymphocyte survival and numbers.

DISCUSSION

In this study, we demonstrate that thymocytes and mature peripheral T cells express all three IP subunits. Although decreased thymocyte numbers were evident in all IP-deficient strains examined, a reduction in peripheral lymphocyte numbers was only seen in LMP2$^{-/-}$ mice. Using progenitor colony assays, BM chimera and lymphocyte transfer, the reduction in

thymocyte and lymphocyte numbers was shown to be not the result of altered progenitor frequency or thymic selection environment but rather intrinsic differences in LMP2$^{-/-}$ thymocytes and lymphocytes. Specifically, at the level of the thymocyte, we found that proteasomes incorporating LMP2 perform important functions to promote lymphocyte survival during β-selection at the DN3 stage, likely by processing and degrading key NFκB and BH3-only protein family members. Given that NFκB signaling is also required during later positive and negative selection [32], we propose that the DN3 stage simply represents the starting point for peripheral T cell deficiency in LMP2$^{-/-}$ mice. Indeed, we found evidence that LMP2-incorporating proteasomes play an important role during mature lymphocyte survival as LMP2$^{-/-}$ lymphocytes showed poor persistence after transfer. This poor survival phenotype was further evident when assessing the phenotype of peripheral T cells, which demonstrated low percentages of memory and high percentages of homeostatically proliferating cells (Figure 3B). We believe this phenotype arises from poor peripheral survival and the remaining cells proliferating unable to fill the available T cell 'niche'. However, restoring the pro-survival/apoptotic balance by either deleting BIM or overexpressing BCL-2 completely reversed this phenotype in LMP2$^{-/-}$ mice. We further demonstrated that the LMP2-containing proteasome is required for degradation of various BH3-only proteins involved in initiating apoptosis and consequently that LMP2-containing proteasomes protect cells from undergoing apoptosis.

One explanation for a reduction of peripheral T cell numbers is the altered thymic selection of maturing thymocytes. Previously, we have shown that LMP2$^{-/-}$ mice have an altered peripheral TCR repertoire that is different from wildtype mice [46]. Despite this, in the example of influenza, LMP2$^{-/-}$ mice still maintain the majority of the influenza-specific TCR repertoire and produce functional T cell responses. From this and that bone marrow chimeric mice (shown in Figure 2A) demonstrate that wild type bone marrow develops normally within a LMP2-deficient thymus, we do not believe a TCR repertoire bias accounts for the phenotype observed in this study, but is instead a non-specific pan-lymphocyte survival deficiency.

As one might predict, part of the phenotypes observed in LMP2$^{-/-}$ mice resemble those in mice deficient in various NFκB family members. For instance, c-REL$^{-/-}$, REL-A$^{-/-}$, p50 and p65 deficient mice all show impaired T and B lymphocyte development [47, 48] due to impaired lymphocyte survival. Of particular relevance to our findings, Mora *et al.* developed an IκBα(ΔN) transgenic mouse, in which IκBα is unable to be degraded and thus prevents functional release of NFκB [35, 49], and observed that T cells showed the same reduction in T

cell number and increase in T cell apoptosis as we observed following loss of LMP2 [35]. Interestingly, these authors also noted a reduction in BCL-2 expression, which might at least in part explain the reduced survival through de-repression of BIM activity. Moreover, given that NFκB signalling has been shown to transcriptionally activate LMP2 [50], it is conceivable that another reason for impaired lymphocyte survival in all of these NFκB family mouse mutants is reduced LMP2 expression and thus relatively higher levels of BIM.

Although the focus of this study was predominantly T cells, our results also indicate a role for the LMP2 subunit in other lymphocyte populations. Adding to our previous description of impaired development in the B cell lineage of LMP2$^{-/-}$ mice [29], here we observed IP expression in the affected B cell developmental stages of LMP2$^{-/-}$ mice (Supplementary figure 2B), indicating that the NFκB pathway and the IP may have a generalized function following antigen receptor signaling. Finally, we found that LMP2$^{-/-}$ B cells have increased levels of BIM and that deletion of BIM or overexpression of BCL-2 restores B cell numbers in LMP2$^{-/-}$ mice (Figure 4E, 5), providing evidence that LMP2 acts to regulate B cell survival via BIM degradation as it does in T cells.

Altered compositions of proteasomes have been reported with highly specialised roles. The 'thymoproteasome' in cTECs, where the β_5 subunit is replaced by the β_{5t} isoform, is postulated to create a unique set of self-peptides presented during positive T cell selection and, consistent with this, β_{5t}-deficient mice display impaired T cell development [51]. Likewise, in the gonads, an alternate α4-like subunit (α4s) was recently described and the resulting 'spermatoproteasome' was required for degradation of histones in mid to late stages of spermatogenesis [52]. Together, these reports suggest that incorporation of specialised subunit isoforms allows the proteasome to fulfil specialised roles.

Until recently, the prevailing dogma was that the housekeeping proteasome and the IP are separate entities, with the former involved in protein processing and recycling [4] and the latter in antigen presentation [53]. Recent research from our group and others indicate that we need to re-think this current paradigm. For example, our demonstration that IP subunits are expressed not just by antigen presenting cells but also by lymphocytes at various developmental stages (Figure 3B and Supplementary figure 2A, B) strongly suggest that antigen processing and presentation is not the sole function of proteasomes incorporating these subunits. Moreover, it is now clear that hybrid proteasomes – consisting of both standard and IP subunits - exist [18, 29] and can potentially account for half the total proteasome content [19]. We postulate that LMP2, LMP7 and LMP10 may each have specialized roles quite separate from their canonical functions as part of the "pure" IP. For instance, our results suggest that the LMP2 subunit –

but not LMP7 or LMP10 - confers unique degradation specificities that promote destruction of crucial pro-apoptotic proteins such as BIM and BAX, and thus offer the best evidence to date of housekeeping roles for the IP. Alternatively, proteasomes incorporating LMP2 may simply be more efficient at protein degradation in general as previously suggested by others [17, 54]. Such efficiency might be an advantage in rapidly developing and proliferating lymphocytes to ensure the timely degradation of key regulatory proteins.

Our results showed that deleting LMP2 in MEFs greatly reduced BIM degradation, which is consistent with the increased BIM expression and apoptosis in LMP2$^{-/-}$ lymphocytes (Figure 4E). As such, we believe the favourable results from the use of Carfilzomib, a treatment of Multiple Myeloma [55], are likely due to either low levels of specificity towards the LMP2 subunit and/or inhibition of the LMP2-incorporated 20s proteasomes. Based on our current findings, we anticipate that a specific LMP2 inhibitor would show greater activity for lymphomas. It would be also interesting to investigate how LMP2 mechanistically improves doxorubicin sensitivity. In this regard, it has been reported that BIM is induced following doxorubicin treatment [56], so conceivably LMP2 inhibition might serve to potentiate this pro-apoptotic effect.

In conclusion, our data indicate a specific role for LMP2 in lymphocyte differentiation and survival that is mediated through modulation of proteins of the NFκB and BH3-only pro-apoptotic pathway. These findings not only emphasize that strict regulation of LMP2 function is required for normal lymphocyte development but more broadly challenge the existing dogma on the biological role of IP subunits. Further studies in this area may help to improve understanding and treatment of human disorders involving disruption or dysregulation of IP subunits, including various cancers for which specific targeting of LMP2 may be a beneficial therapeutic strategy.

METHODS

Animals

All animal experimentation was approved and in accordance with the Austin Health and La Trobe University Animal Ethics Committee guidelines and used six- to eight-week-old female mice. C57BL/6J (B6) mice were purchased from Walter Eliza Hall Institute of Medical Research (Kew, Australia). F5 mice [57] carrying transgenic TCR specific for $NP_{366-374}$ of A/NT/60/68 (NT60) were bred onto LMP2$^{-/-}$ mice to derive LMP2$^{-/-}$-F5. Proteasome subunit deficient mice were reported previously [15]. vav-BCL-2-Tg mouse was a gift from Prof. Jerry Adams (WEHI). To establish LMP2$^{-/-}$BCL-2$^{+/-}$ mice, six-to-eight week old

heterozygous vav-BCL-$2^{+/-}$ transgenic (vav-BCL-2-Tg) [45] males on B6 background were crossed with age-matched $LMP2^{-/-}$ female mice. $LMP2^{+/-}$ $BCL\text{-}2^{+/-}$ F1 males were again back crossed with $LMP2^{-/-}$ females to generate $LMP2^{-/-}BCL\text{-}2^{+/-}$ female mice. Genotypes of the mice were confirmed by PCR for both LMP2 and BCL-2 genes to define a 200bp PCR fragment for human BCL-2; wild type LMP2 gene to detect a 360bp PCR fragment and knockout LMP2 gene to detect a 170bp PCR fragment. $BIM^{-/-}$ mice were a kind gift of Philippe Bouillet (WEHI) and have been described previously [58]. To establish $LMP2^{-/-}BIM^{-/-}$ mice, six- to eight-week-old heterozygous $BIM^{+/-}$ males on B6 background were crossed with age-matched $LMP2^{-/-}$ female mice. $LMP2^{+/-}$ $BIM^{+/-}$ F1 litter mates were crossed to generate $LMP2^{-/-}BIM^{-/-}$ female mice. Genotypes of the mice were confirmed by PCR for both LMP2 and BIM genes to detect a 500bp (wt) or 620bp (KO) PCR fragment; as described earlier LMP2 genotyping was determined by PCR analysis of genomic DNA samples using wild type and knockout LMP2 primer sets. All primers are described in Supplementary figure 3A. Mice were bred and housed under specific pathogen free conditions. Spleen, thymus, lymph nodes and femurs were collected into RF-10 (RPMI-1640 containing 10% FCS).

Generation of BM chimeric mice

Recipient mice were exposed to 2 x 500 Rads in a Gammacell® 1000 Elite Irradiator, separated by a 60-minute interval. 5 x 10^6 donor bone marrow (BM) cells were injected i.v. Recipient mice were injected with 50 μg T24 monoclonal antibody (mAb) i.p to deplete radio-resistant T cells. All chimeric mice were given water containing Neomycin sulfate (25 mg/l) and Polymyxin B sulfate (13 mg/l) for 2 weeks following BM reconstitution.

Cell lines

OP9-DL1 cells were cultured in Alpha-MEM containing 1 mM L-Glutamine, 100 U mL^{-1} penicillin and 100 μg mL^{-1} streptomycin, 10 mM HEPES, 1 mM Sodium pyruvate, 50 μM 2-Mercaptoethanol,containing 20% FCS. thymocyte culture methods and OP9 limiting dilution B cell CFAs have been described previously [33]. Mouse embryonic fibroblasts were cultured in DMEM containing 10% FCS, 50μm 2-Mercaptoethanol, 2mM L-glutamine, 100U mL^{-1} penicillin and 100μg mL^{-1} streptomycin. Human Myeloma cell lines RPMI-8226, U226, NCI-H929 and LP-1 were cultured in RPMI-1640 containing 10% FCS, 50 μM 2-Mercaptoethanol, 2 mM L-glutamine, 100 U mL^{-1} penicillin and 100 μg mL^{-1} streptomycin. All cell lines were cultured at 37°C 5% CO_2.

Primary cell culture

Ex vivo isolated cells from female mice were cultured in RPMI-1640 containing 10% FCS, 50 μM 2-Mercaptoethanol, 2 mM L-glutamine, 100 U mL^{-1} penicillin and 100 μg mL^{-1} streptomycin at 37°C 5% CO_2. Cultures involving splenic T cells additionally included 10U IL-2 mL^{-1}.

Antibodies

Cell phenotyping markers are described in Supplementary table 2 and were typically used at 1:300 dilution in PBS containing 10% FCS, incubated for 30 minutes at 4 °C and washed with PBS before analysis by flow cytometry. Western blotting primary antibodies were typically used at 1:1000 dilution in TBS/T containing 5% BSA as per manufacturer's instructions.

$BIM^{-/-}$ BIM_{EL} and CRISPR/ CAS9 LMP2-subunit knockout mouse embryonic fibroblasts

Generation of $BIM^{-/-}$ mouse embryonic fibroblasts (MEFs) expressing wild type BIM under 4-hydroxytamoxefen has been previously described [42]. CRISPR knockout MEFs were generated as described previously [59]. CRISPR guides were generated according to the MIT algorithm (http://crispr.mit.edu/). Three guide RNA sequences targeting LMP2 were utilised. Guide sequences are given in Supplementary figure 3. Lentivirally infected cells were sorted on a FACS AriaIII and deletions in clones were induced by adding 1 μg mL^{-1} doxycycline hyclate (D9891-5G, Sigma-Aldrich, NSW, Australia). Clones with gene specific deletions were confirmed by WB analysis (Supplementary figure 3).

CFSE and eFluor® 670 labeling, apoptosis staining and cell sorting

Cells were labeled with 2.5 μM CFSE for 10 minutes at 37°C and washed three times before further use. Cells were labeled with 5 μM eFluor®670 (eBiosciences, USA) for 10 minutes at 37°C and washed three times before further use. Apoptosis staining was conducted using the Vybrant Assays Apoptosis Kit # 8 (Invitrogen). Cell sorting was conducted either on a MoFlo® (DakoCytomation, USA) or FACS AriaIII™ (Becton Dickinson, USA) instrument.

Western blot

Cells were then lysed in RIPA buffer on ice for 15 minutes, sonicated for 15 minutes and cell debris pelleted by centrifugation. Samples followed standard Western blotting procedure [15].

OP9-DL1 thymocyte culture

OP9-DL1 thymocyte culture methods have been described previously [33]. BM cells were depleted of lineage positive populations using an EasySep Magnetic depletion kit (StemCell Technologies, USA) to isolate hematopoietic stem cells (HSCs).

T cell co-transfer and tracking analysis

FACS-sorted, CFSE and eFluor®670 labeled splenic T_{CD8+} from Ly5.1-F5 and LMP2$^{-/-}$-F5, or T_{CD8+} from B6-vav-BCL-2-Tg, LMP2$^{-/-}$-vav-BCL-2-Tg, BIM$^{-/-}$, LMP2$^{-/-}$ BIM$^{-/-}$ or LMP2$^{-/-}$ mice were mixed at a ratio of 1:1 and a total of 5 x 10^6 cells were transferred i.v into individual recipient mice. Transferred cells were recovered after 7 days from the entire secondary lymphoid compartment and enumerated by FACs.

Quantification and statistical analysis

All data are representative of minimum two independent experiments. All error bars represent standard error of the mean using a sample size 6 per group. N = 6 mice per group for all *ex vivo* experiments. Unless otherwise specified, statistical analyses were performing using either a Student's *t*-test or a one-way ANOVA followed by Bonferroni's post-hoc comparison test, with a *P*- value threshold of < 0.05 considered statistically significant.

AUTHOR CONTRIBUTIONS

DZ and KP designed, performed experiments and wrote the manuscript. SO, CL, PF, GM, CN and CQ performed experiments. SC, GK, MH, SN and PN provided experimental reagents. HP and WC designed experiments and wrote the manuscript.

ACKNOWLEDGMENTS

This project was partly supported by the NHMRC project grants 433608 and 542508 to WC and the NHMRC program grant 567122. DZ was supported by NHMRC biomedical postgraduate scholarship 487926. SLN, MLH and WC are NHMRC Senior Research Fellows. SC is supported by an NHMRC Career Development Award, SLN by an Australian Research Council Future Fellowship and KP is supported by a Melbourne Children's Clinician Scientist

Fellowship. The Walter and Eliza Hall Institute is supported by Victorian State Government Operational Infrastructure Support and an Australian Government NHMRC IRIIS.

CONFLICT OF INTEREST

The authors declare no conflict of interest.

REFERENCES

1. Ciechanover A. *Proteolysis: from the lysosome to ubiquitin and the proteasome*. Nature reviews Molecular cell biology. 2005;**6**:79-87.

2. Voges D, Zwickl P, Baumeister W. *The 26S proteasome: A molecular machine designed for controlled proteolysis*. Annu Rev Biochem. 1999;**68**:1015-1068.

3. Basak S, Kim H, Kearns JD*, et al. A fourth IkappaB protein within the NF-kappaB signaling module*. Cell. 2007;**128**:369-381.

4. York LA, Goldberg AL, Mo XY*, et al. Proteolysis and class I major histocompatibility complex antigen presentation*. Immunol Rev. 1999;**172**:29-48.

5. McMichael AJ, Gotch FM, Noble GR*, et al. Cytotoxic T-cell immunity to influenza*. N Engl J Med. 1983;**309**:13-17.

6. Groll M. *Structure of 20S proteasome from yeast at 2.4 A resolution*. Nature. 1997;**386**:463-741.

7. Ortiz-Navarette V. *Subunit of the 20S proteasome (multicatalytic proteinase) encoded by the major histocompatibility complex*. Nature. 1991;**353**:662-664.

8. Glynne R. *A proteasome related gene between the two ABC transporter loci in the class II region of the human MHC*. Nature. 1991;**353**:357-360.

9. Driscoll J, Brown MG, Finley D*, et al. MHC-linked LMP gene products specifically alter peptidase activities of the proteasome*. Nature. 1993;**365**:262-264.

10. Groettrup M, Standera S, Stohwasser R*, et al. The subunits MECL-1 and LMP2 are mutually required for incorporation into the 20S proteasome*. Proc Natl Acad Sci U S A. 1997;**94**:8970-8975.

11. Nil A, Firat E, Sobek V*, et al. Expression of housekeeping and immunoproteasome subunit genes is differentially regulated in positively and negatively selecting thymic stroma subsets*. Eur J Immunol. 2004;**34**:2681-2689.

12. Aki M, Shimbara N, Takashina M*, et al. Interferon-gamma induces different subunit organizations and functional diversity of proteasomes*. Journal of biochemistry. 1994;**115**:257-269.

13. Falk K, Rotschke O, Stevanovic S*, et al. Allele-specific motifs revealed by sequencing of self-peptides eluted from MHC molecules*. Nature. 1991;**351**:290-296.

14. Gacynska M, Rock KL, Goldberg AL. *Gamma interferon and expression of MHC genes regulate peptide hydrolysis*. Nature. 1993;**363**:262-264.

15. Pang KC, Sanders MT, Monaco JJ*, et al. Immunoproteasome subunit deficiencies impact differentially on two immunodominant influenza virus-specific CD8+ T cell responses*. J Immunol. 2006;**177**:7680-7688.

16. Zanker D, Waithman J, Yewdell JW*, et al. Mixed proteasomes function to increase viral peptide diversity and broaden antiviral CD8+ T cell responses*. J Immunol. 2013;**191**:52-59.

17. Mishto M, Liepe J, Textoris-Taube K*, et al. Proteasome isoforms exhibit only quantitative differences in cleavage and epitope generation*. Eur J Immunol. 2014e-pub ahead of print Sep 17;10.1002/eji.201444902.

18. Drews O, Wildgruber R, Zong C*, et al. Mammalian proteasome subpopulations with distinct molecular compositions and proteolytic activities*. Molecular & cellular proteomics : MCP. 2007;**6**:2021-2031.

19. Guillaume B, Chapiro J, Stroobant V*, et al. Two abundant proteasome subtypes that uniquely process some antigens presented by HLA class I molecules*. Proc Natl Acad Sci U S A. 2010;**107**:18599-18604.

20. Kanazawa N. *Nakajo-Nishimura syndrome: an autoinflammatory disorder showing pernio-like rashes and progressive partial lipodystrophy*. Allergology international : official journal of the Japanese Society of Allergology. 2012;**61**:197-206.

21. Seifert U, Bialy LP, Ebstein F*, et al. Immunoproteasomes preserve protein homeostasis upon interferon-induced oxidative stress*. Cell. 2010;**142**:613-624.

22. Bianchi G, Oliva L, Cascio P*, et al. The proteasome load versus capacity balance determines apoptotic sensitivity of multiple myeloma cells to proteasome inhibition*. Blood. 2009;**113**:3040-3049.

23. Diaz-Hernandez M, Hernandez F, Martin-Aparicio E*, et al. Neuronal induction of the immunoproteasome in Huntington's disease*. The Journal of neuroscience : the official journal of the Society for Neuroscience. 2003;**23**:11653-11661.

24. Mishto M, Bellavista E, Santoro A*, et al. Immunoproteasome and LMP2 polymorphism in aged and Alzheimer's disease brains*. Neurobiology of aging. 2006;**27**:54-66.

25. Ma X, Yang C, Tang R*, et al. Association between LMP2 and LMP7 gene polymorphisms and the risk of gastric cancer: A case-control study*. Oncology letters. 2015;**10**:509-517.

26. Puttaparthi K, Elliott JL. *Non-neuronal induction of immunoproteasome subunits in an ALS model: possible mediation by cytokines*. Experimental neurology. 2005;**196**:441-451.

27. Van Kaer L. *Altered peptidase and viral-specific T cell response in LMP2 mutant mice*. Immunity. 1994;**1**:533-541.

28. Zaiss DM, de Graaf N, Sijts AJ. *The proteasome immunosubunit multicatalytic endopeptidase complex-like 1 is a T-cell-intrinsic factor influencing homeostatic expansion*. Infect Immun. 2008;**76**:1207-1213.

29. Hensley SE, Zanker D, Dolan BP*, et al. Unexpected role for the immunoproteasome subunit LMP2 in antiviral humoral and innate immune responses*. J Immunol. 2010;**184**:4115-4122.

30. Kondo M, Weissman IL, Akashi K. *Identification of clonogenic common lymphoid progenitors in mouse bone marrow*. Cell. 1997;**91**:661-672.

31. Akashi K, Traver D, Miyamoto T*, et al. A clonogenic common myeloid progenitor that gives rise to all myeloid lineages*. Nature. 2000;**404**:193-197.

32. Siebenlist U, Brown K, Claudio E. *Control of lymphocyte development by nuclear factor-kappaB*. Nat Rev Immunol. 2005;**5**:435-445.

33. Schmitt TM, Zuniga-Pflucker JC. *Induction of T cell development from hematopoietic progenitor cells by delta-like-1 in vitro*. Immunity. 2002;**17**:749-756.

34. Fiorini E, Schmitz I, Marissen WE*, et al. Peptide-induced negative selection of thymocytes activates transcription of an NF-kappa B inhibitor*. Mol Cell. 2002;**9**:637-648.

35. Mora AL, Corn RA, Stanic AK*, et al. Antiapoptotic function of NF-kappaB in T lymphocytes is influenced by their differentiation status: roles of Fas, c-FLIP, and Bcl-xL*. Cell Death Differ. 2003;**10**:1032-1044.

36. Murali-Krishna K, Ahmed R. *Cutting edge: naive T cells masquerading as memory cells*. J Immunol. 2000;**165**:1733-1737.

37. Dimmeler S, Breitschopf K, Haendeler J*, et al. Dephosphorylation targets Bcl-2 for ubiquitin-dependent degradation: a link between the apoptosome and the proteasome pathway*. J Exp Med. 1999;**189**:1815-1822.

38. Li B, Dou QP. *Bax degradation by the ubiquitin/proteasome-dependent pathway: involvement in tumor survival and progression*. Proc Natl Acad Sci U S A. 2000;**97**:3850-3855.

39. Korsmeyer SJ, Wei MC, Saito M*, et al. Pro-apoptotic cascade activates BID, which oligomerizes BAK or BAX into pores that result in the release of cytochrome c*. Cell Death Differ. 2000;**7**:1166-1173.

40. Lomonosova E, Ryerse J, Chinnadurai G. *BAX/BAK-independent mitoptosis during cell death induced by proteasome inhibition?* Molecular cancer research : MCR. 2009;**7**:1268-1284.

41. Bouillet P, Purton JF, Godfrey DI*, et al. BH3-only Bcl-2 family member Bim is required for apoptosis of autoreactive thymocytes*. Nature. 2002;**415**:922-926.

42. Moujalled D, Weston R, Anderton H*, et al. Cyclic-AMP-dependent protein kinase A regulates apoptosis by stabilizing the BH3-only protein Bim*. EMBO reports. 2011;**12**:77-83.

43. Breitschopf K, Zeiher AM, Dimmeler S. *Ubiquitin-mediated degradation of the proapoptotic active form of bid. A functional consequence on apoptosis induction*. J Biol Chem. 2000;**275**:21648-21652.

44. Puthalakath H, O'Reilly LA, Gunn P*, et al. ER stress triggers apoptosis by activating BH3-only protein Bim*. Cell. 2007;**129**:1337-1349.

45. Ogilvy S, Metcalf D, Print CG*, et al. Constitutive Bcl-2 expression throughout the hematopoietic compartment affects multiple lineages and enhances progenitor cell survival*. Proc Natl Acad Sci U S A. 1999;**96**:14943-14948.

46. Chen W, Norbury CC, Cho Y*, et al. Immunoproteasomes shape immunodominance hierarchies of antiviral CD8(+) T cells at the levels of T cell repertoire and presentation of viral antigens*. J Exp Med. 2001;**193**:1319-1326.

47. Horwitz BH, Scott ML, Cherry SR*, et al. Failure of lymphopoiesis after adoptive transfer of NF-kappaB-deficient fetal liver cells*. Immunity. 1997;**6**:765-772.

48. Grossmann M, O'Reilly LA, Gugasyan R*, et al. The anti-apoptotic activities of Rel and RelA required during B-cell maturation involve the regulation of Bcl-2 expression*. EMBO J. 2000;**19**:6351-6360.

49. Brockman JA, Scherer DC, McKinsey TA*, et al. Coupling of a signal response domain in I kappa B alpha to multiple pathways for NF-kappa B activation*. Mol Cell Biol. 1995;**15**:2809-2818.

50. Wright KL, White LC, Kelly A*, et al. Coordinate regulation of the human TAP1 and LMP2 genes from a shared bidirectional promoter*. J Exp Med. 1995;**181**:1459-1471.

51. Murata S, Sasaki K, Kishimoto T*, et al. Regulation of CD8+ T cell development by thymus-specific proteasomes*. Science. 2007;**316**:1349-1353.

52. Qian MX, Pang Y, Liu CH*, et al. Acetylation-mediated proteasomal degradation of core histones during DNA repair and spermatogenesis*. Cell. 2013;**153**:1012-1024.

53. Strehl B, Textoris-Taube K, Jakel S*, et al. Antitopes define preferential proteasomal cleavage site usage*. J Biol Chem. 2008;**283**:17891-17897.

54. Sijts A. *Structural features of immunoproteasomes determine the efficient generation of a viral CTL epitope*. J Exp Med. 2000;**191**:503-513.

55. Shah JJ, Orlowski RZ. *Proteasome inhibitors in the treatment of multiple myeloma*. Leukemia. 2009;**23**:1964-1979.

56. Schneider-Jakob S, Corazza N, Badmann A*, et al. Synergistic induction of cell death in liver tumor cells by TRAIL and chemotherapeutic drugs via the BH3-only proteins Bim and Bid*. Cell death & disease. 2010;**1**:e86.

57. Mamalaki C, Elliott J, Norton T*, et al. Positive and negative selection in transgenic mice expressing a T-cell receptor specific for influenza nucleoprotein and endogenous superantigen*. Developmental immunology. 1993;**3**:159-174.

58. Bouillet P, Metcalf D, Huang DC*, et al. Proapoptotic Bcl-2 relative Bim required for certain apoptotic responses, leukocyte homeostasis, and to preclude autoimmunity*. Science. 1999;**286**:1735-1738.

59. Aubrey BJ, Kelly GL, Kueh AJ*, et al. An inducible lentiviral guide RNA platform enables the identification of tumor-essential genes and tumor-promoting mutations in vivo*. Cell reports. 2015;**10**:1422-1432.

FIGURE LEGENDS

Figure 1. LMP2$^{-/-}$ mice exhibit reduced lymphocyte numbers. (a) Cell numbers were enumerated from the thymus, spleen and BM of LMP2$^{-/-}$, LMP7/LMP10$^{-/-}$, LMP10$^{-/-}$ and B6 mice. **(b)** Splenic subset cell numbers. Cell phenotyping markers are described in Supplementary table 2. One-way ANOVA followed by Bonferroni's post-hoc comparison test and SEM values shown *P < 0.05. Data are combination of three independent experiments. N= 12 mice/ group.

Figure 2. Reduced lymphocyte number is an intrinsic defect as a result of LMP2$^{-/-}$ deficiency. (a) BM cells from wild type or LMP2$^{-/-}$ mice were transferred into irradiated wild type or LMP2$^{-/-}$ recipients. Following 3 months of reconstitution, splenic donor cell subsets were analyzed via FACs. One-way ANOVA followed by Bonferroni's post-hoc comparison test and SEM values shown * P < 0.05. Data are combination of two independent experiments. N= 6 mice/ group. **(b)** Mixed BM chimeras: BM cells were isolated from LMP2$^{-/-}$ and Ly5.1^{+} mice and co-transferred into irradiated Thy1.1^{+} recipients at 1:1 (LMP2$^{-/-}$:Ly5.1^{+}) or 5:1 ratios. Following 3 months of reconstitution, donor total T cell percentages were analyzed in the thymus and spleen. **(c)** Lin^{-ve} cells were stained for c-kit and Sca-1, and

HSC, CMP and CLP cell numbers were calculated by FACs. **(d)** Thymocytes from LMP2$^{-/-}$ and B6 mice were stained for thymic development subset markers and analyzed via FACs. Student's *t*-test and SEM values shown * $P < 0.05$. Data are combination of two independent experiments. N= 6 mice/ group.

Figure 3. LMP2$^{-/-}$ T_{CD8+} display homeostatic proliferation properties, yet decreased *in vivo* survival and pro-apoptotic phenotype. (a) Splenic T_{CD8+} from B6, LMP2$^{-/-}$, LMP7/LMP10$^{-/-}$ and LMP10$^{-/-}$ mice were sorted and expression of IP subunits (LMP2, LMP7, LMP10) assessed via WB analysis (loading control: GAPDH; 5 x 10^5 cells /lane). Data are one representative of three independent experiments. **(b)** Splenic T_{CD8+} from B6 and LMP2$^{-/-}$ mice were assessed for expression of CD44 and CD62L via FACs; i: naïve, ii: central memory /homeostatically proliferating, iii: effector memory. **(c)** T_{CD8+} were isolated from Ly5.1-F5 TCR Tg and LMP2$^{-/-}$-F5 TCR Tg mice, labeled with CFSE or eFluor®670 and 5 x 10^6 cells (1:1 ratio) transferred i.v into WT or LMP2$^{-/-}$ recipients. 7 days post transfer, peritoneal exudates, lymph nodes and spleen were pooled and donor cells were enumerated: Ly5.1-F5 (CD45.1$^+$), LMP2$^{-/-}$-F5 (CD45.2$^+$). Data are combination of two independent experiments. N= 6 mice/ group. **(d)** Splenic T_{CD8+} from B6 and LMP2$^{-/-}$ mice were cell sorted and Annexin V$^+$ and Sytox Green$^+$ cells were enumerated and characterized into live, early and late apoptotic subsets. Data an average of 3 biological replicates. Student's *t*-test and SEM values shown * $P < 0.05$.

Figure 4. LMP2-deficient proteasome has altered degradation of BH3-only proteins. (a) Wild type BIM$^{-/-}$BIM$_{EL}$ and LMP2$^{-/-}$BIM$^{-/-}$BIM$_{EL}$ MEFs were incubated in the presence of IFN-γ for 48hrs. MEFs were then incubated in the presence of 5nM 4-hydroxytamoxifen for 16hrs to induce BIM$_{EL}$ expression. MEFs were then incubated in the presence of Cycloheximide and degradation of BIM was assessed from 0 to 4hrs. Cells were lysed and BIM$_{EL}$ protein level was assessed via WB. **(b)** Quantification of BIM$_{EL}$ expression from (a). **(c)** BAX and **(d)** t-BID levels were assessed in a similar manner. **(e)** 1 x 10^6 B cells and T_{CD8+} from LMP2$^{-/-}$ and B6 mice were FACS sorted, lysed and BIM, BAX, and BAK protein levels were assessed via WB. Data are one representative of three independent experiments.

Figure 5. BCL-2 Transgene or BIM-deletion corrects LMP2$^{-/-}$ lymphopenia. (a) Cell numbers were enumerated from the thymus, spleen and BM of B6, LMP2$^{-/-}$, BIM$^{-/-}$, LMP2$^{-/-}$

$BIM^{-/-}$, B6-vav-BCL-2-Tg, and $LMP2^{-/-}$-vav-BCL-2-Tg mice. **(b)** Splenic cells of these mice were analyzed by FACS for B cells, CD4+ and CD8+ T cells. **(c)** T_{CD8+} were isolated from; Group 1: $LMP2^{-/-}$ and $BIM^{-/-}$; Group 2: $LMP2^{-/-}$ and $LMP2^{-/-}BIM^{-/-}$; or Group 3: $BIM^{-/-}$ and $LMP2^{-/-}BIM^{-/-}$ mice, and **(d)** T_{CD8+} were isolated from; Group 1: $LMP2^{-/-}$ and B6-vav-BCL-2-Tg; Group 2: $LMP2^{-/-}$ and $LMP2^{-/-}$-vav-BCL-2-Tg; or Group 3: $LMP2^{-/-}$-vav-BCL-2-Tg and B6-vav-BCL-2-Tg mice, labeled with CFSE or eFluor670 dye and 5 x 10^6 cells (1:1 ratio) transferred i.v into $CD45.1^+$ recipients. 7 days post transfer, peritoneal exudates, lymph nodes and spleen were harvested and donor cells enumerated. One-way ANOVA followed by Bonferroni's post-hoc comparison test or student's *t*-test and SEM values shown * $P < 0.05$. Data are combination of two independent experiments. N= 6 mice/ group.

SUPPLEMENTARY FILES

Supplementary table 1: BM chimera experimental groups.

Supplementary table 2: Cell phenotyping markers.

Supplementary figure 1. $LMP2^{-/-}$ mice have impaired *in vitro* progression to thymic DP stage. (a) Size and cell number of e*x vivo* isolated DN3 thymocytes were assessed (E: expected size, L: large size). **(b-d)** HSCs taken from $LMP2^{-/-}$ and B6 BM were cultured with OP9-DL1 feeder cells in medium containing IL-7 and Flt-3L. Following 15 days of culture, cells were analyzed for thymic differentiation stage via FACs. Quantification of DP thymocytes are shown in **(b)**, while representative FACs plots showing DP cells and DN cell stages are shown in **(c)** and **(d)** respectively. DN cell phenotyping markers are described in Table S2. N= 6 mice/ group. **(e)** B6 and $LMP2^{-/-}$ thymocytes were CFSE labeled and cultured in the presence of 1ug mL^{-1} Concanavalin A for 72hrs. **(f)** Thymocytes from $LMP2^{-/-}$ and B6 mice were stained for apoptotic marker Annexin V. N= 6 mice/ group. Data are one representative of three independent experiments. Student's *t*-test and SEM values shown * $P < 0.05$.

Supplementary figure 2. Developing lymphocytes express immunoproteasome subunits during stages of antigen-receptor interrogation. LMP2$^{-/-}$-F5 TCR Tg mice exhibit similar lymphopenia to that in LMP2$^{-/-}$ mice. (a) Thymocyte DN3 and DN4 and **(b)** bone marrow pre-B and Immature B cell subsets were lysed and analysed by western blot for immunoproteasome subunits. **(c)** Thymi were isolated from Ly5.1-F5 TCR Tg and LMP2$^{-/-}$-F5 TCR Tg mice and various thymic subsets were enumerated by FACs. **(d)** Splenic subsets from Ly5.1-F5 TCR Tg and LMP2$^{-/-}$-F5 TCR Tg mice were analyzed by FACs. N= 6 mice/ group. **(e)** BM cells from LMP2$^{-/-}$ mice were transferred into irradiated wild type or LMP2$^{-/-}$ recipients. Following 3 months of reconstitution, splenic donor cell subsets were analyzed via FACs for CD8, CD44 and CD62L. Data are one representative of three independent experiments. Student's *t*-test and SEM values shown * $P < 0.05$.

Supplementary figure 3. CRISPR/ Cas9 deletion validation. (a) gRNA sequences used for targeted deletion of IP subunits in MEFs. Various CRISPR/ Cas9 gRNA treated BIM$^{-/-}$ BIM_{EL} MEF clones were assessed for deletion of **(b)** LMP2. Deletion success rate was 16% for LMP2 (3/19 clones).

Figure 1

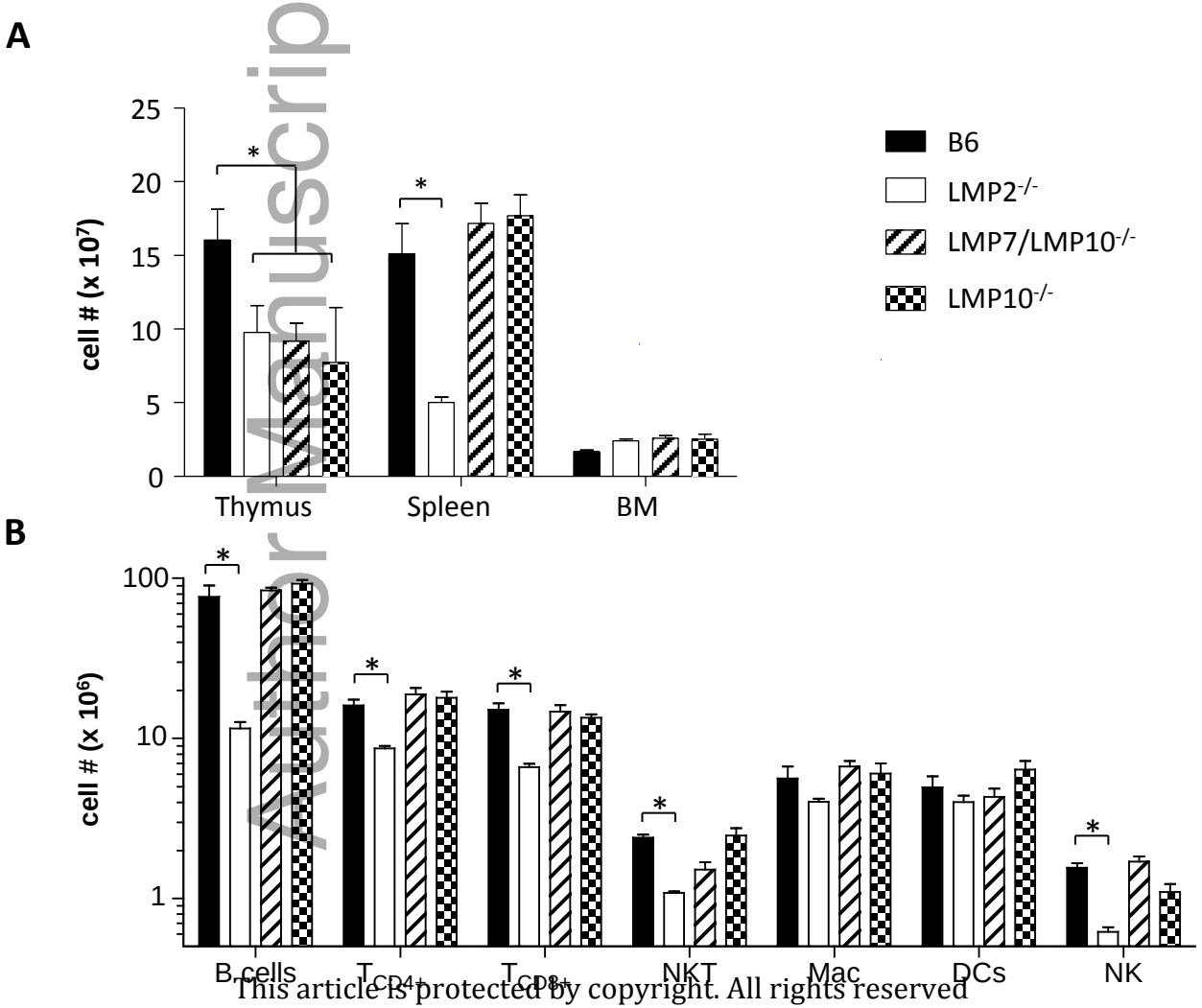

Figure 2

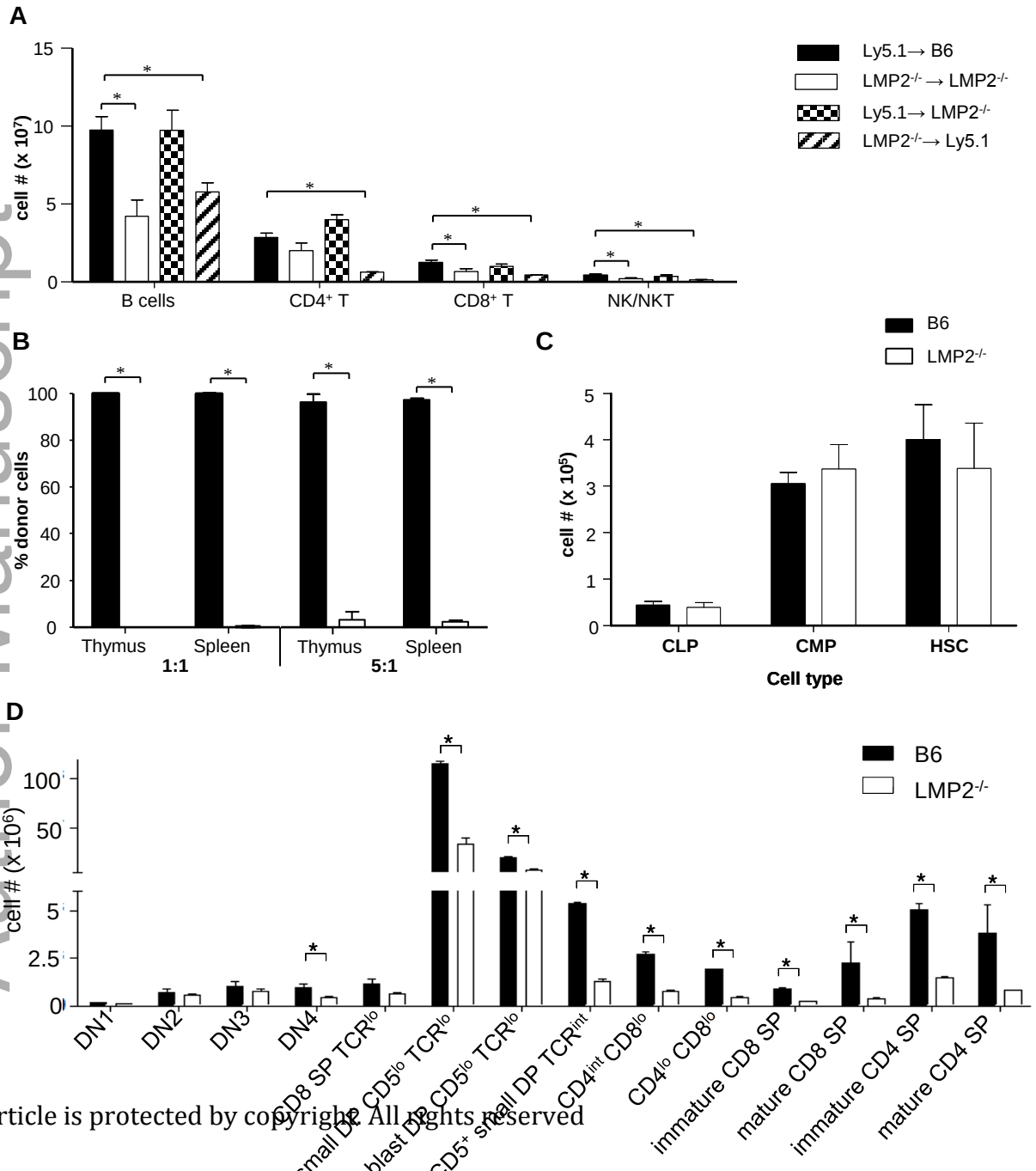

Figure 3

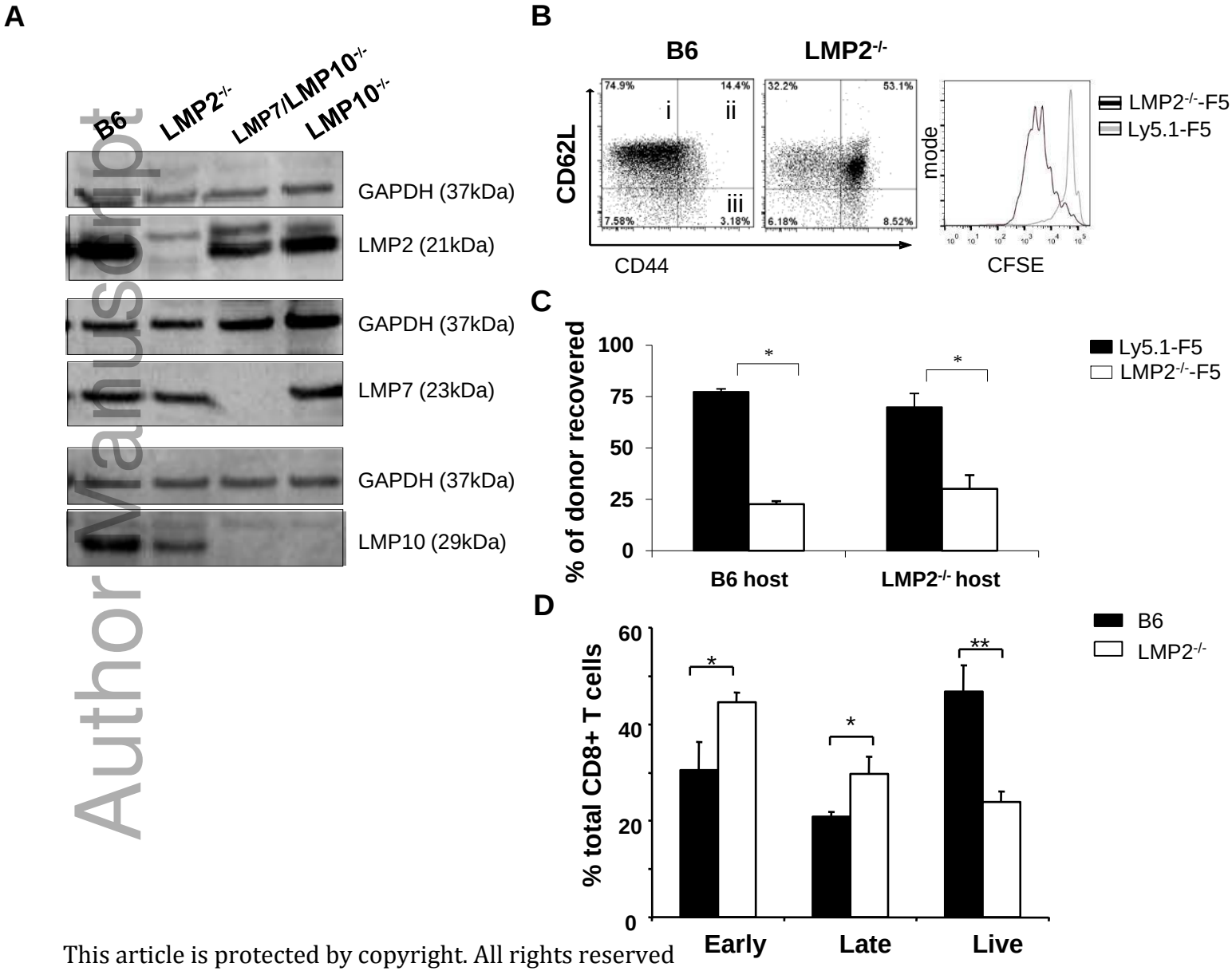

Figure 4

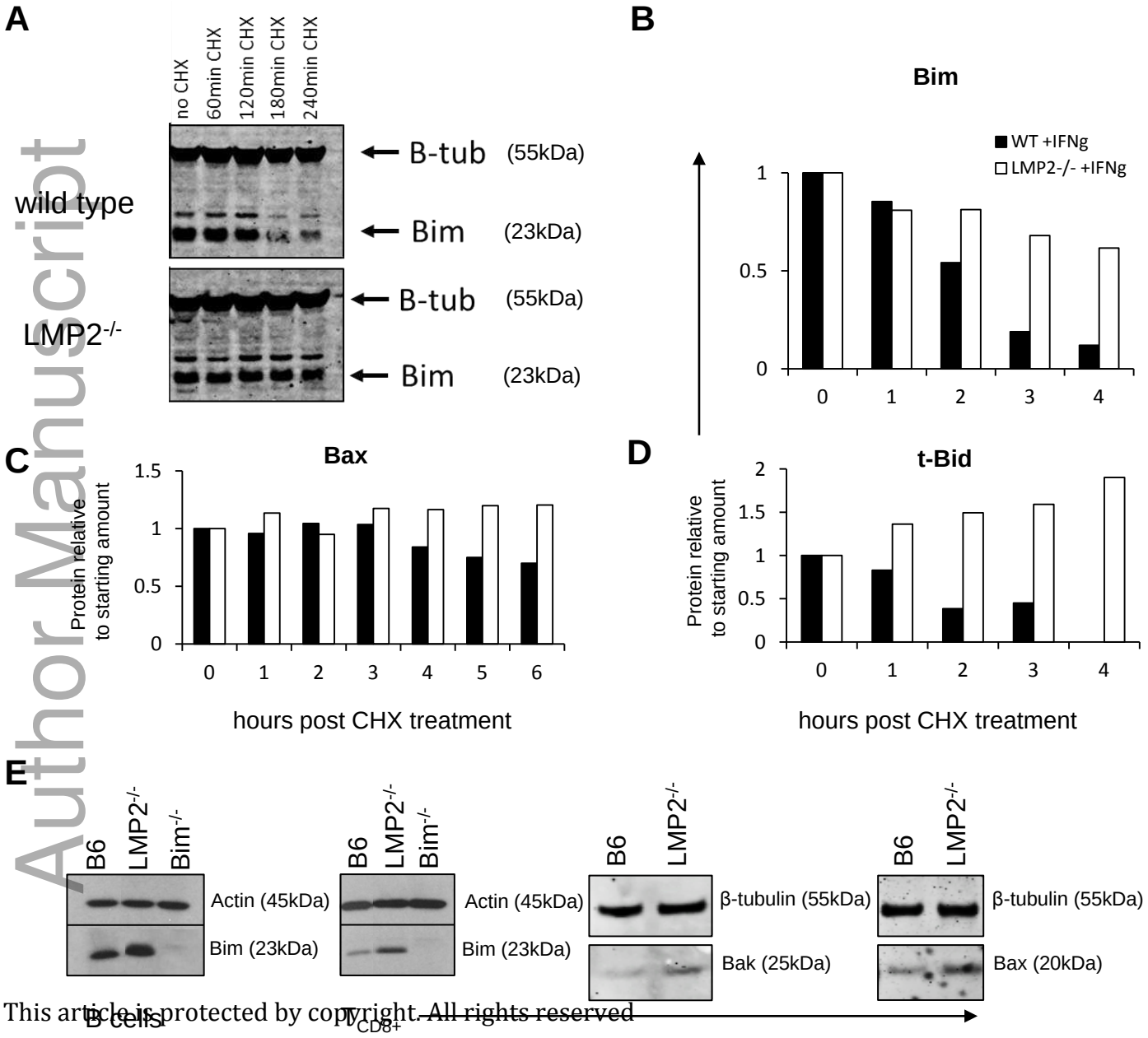

Figure 5